International Journal of Frontiers in
Life Science Research
Journal homepage: https://frontiersrj.com/journals/ijflsr/
ISSN: 2783-0470 (Online)

(RESEARCH ARTICLE)

Check for updates

Performance modelling of an electric vapor compression solar refrigeration system (SE-VCR) case for Madagascar

Rakotondrazano Yvon [1], Modeste Kameni Nematchoua [1, 2, 3, *] and RAMINOSOA Chrysostome [1]

[1] *Fluid and Energy Laboratory, University of Antisana, Madagascar.*
[2] *Laboratory of Energy and Environment, Faculty of Sciences, University of Yaounde1, Cameroun.*
[3] *Local Environment Management & Analysis (LEMA), Department of Architecture, Geology, Environment and Constructions, Allée de la Découverte 9, Quartier Polytech 1, BE-4000 Liège, Belgium.*

International Journal of Frontiers in Life Science Research, 2021, 01(02), 028–051

Publication history: Received on 20 October 2021; revised on 28 November 2021; accepted on 30 November 2021

Article DOI: https://doi.org/10.53294/ijflsr.2021.1.2.0057

Abstract

This study presents an evaluation of the performance of an electric vapor compression solar refrigeration system coupled with solar energies for the different climatic zones in Madagascar. For the 5 selected cities, a building of the same constructive design was used. Hourly building heat loads were estimated from the heat balance method using meteorological data from selected cities such as hourly average solar radiation and atmospheric temperatures. Then, the hourly evaluation of various parameters such as the coefficient of performance, the capacity of the condenser, the electrical consumption of the compressor and the power of the photovoltaic generators as well as its surface for different evaporation temperatures were determined. It was determined that the SE-VCR system could be used successfully for the province of Mahajanga, Antsiranana, Toliara and Tamatave while for the city of Antananarivo was not very interesting.For these 4 cities, the coefficient of performance varies from around 3.3 to 4.43 for an evaporation temperature Te = 0 ° C. And the power of the compressor varies from 5.66 to 7.5 kW with a peak power of the solar panels varying from 21.16 to 25.23 kWp with a respective surface of 104.93 to 125.12 m^2. The overall efficiency of the installation varies from 0.483 to 0.521.

Keywords: Solar refrigeration; SE-VCR system; Thermal comfort; Renewable energies; Madagascar Tropical regions

1. Introduction

Since the end of the 1980s, the international scientific community has been interested in global climate change and questions its future impacts on the planetary scale. The various reports of the IPCC (Intergovernmental Panel on Climate Change) have alerted the international community to an increase in temperature as well as the frequency and intensity of climatic hazards at the global level (IPCC, 1990, 1995, 2001, 2007 and 2014). According to climate model projections based on all the considered greenhouse gas emission scenarios carried out by the IPCC in its last part of the fifth assessment report in 2014 [1], it indicates an increase in surface temperature of the globe from 3.7 to 4.8 ° C until the end of the 21st century. In the same report, he claims 95% that human is the primary cause of current global warming.

This phenomenon implies strong human and environmental consequences in the medium and long term. Therefore, realizing the gravity of the situation, the world community decided to take initiatives to limit the process. One of the most famous in force happens to be the Kyoto Protocol [2,3]. This is an international treaty requiring industrialized countries to reduce their greenhouse gas emissions by 5.2% compared to 1990. The refrigeration industry is one of the

* Corresponding author: Modeste Kameni Nematchoua
Fluid and Energy Laboratory, University of Antsiranana, Madagascar.

most affected. by this protocol because of the significant impact of refrigerants on the environment. For example, in Europe, the use of HFC-134a will be prohibited from 2015, whether in new or old installations [3,4].

During the last decade, the increase in the standard of living, the reinforcement of the insulation of buildings (Thermal Regulations), a demand for increased comfort and the increase in summer temperatures have led to a strong development of air conditioning, with the development of the global economy, energy consumption in buildings has increased and represents 30% of the total energy used. [3, 5,6]. Today, the building sector is responsible for a quarter of greenhouse gas emissions [3, 5,6]. Gradually, the contribution of renewable energies becomes essential to achieve the reduction objectives set by the various authorities.

To avoid these human and environmental impacts, we must reduce greenhouse gas emissions resulting from the combustion of fossil fuels as an energy source. Faced with this problem, resorting to renewable energies is one of the more practical, clean and sustainable solutions. Among renewable energy sources, solar energy is the most important and attractive source; due to its universal abundance and limitless nature unlike many other renewable energy sources [7]. The attractive feature of solar power is that the continuous source is endless even though it is an intermittent source during the day and night. In addition, solar energy does not cause air pollution and does not affect the earth's surface as a fossil fuel. Solar energy is easy to harness unlike the extraction of fossil fuels. Solar cooling technologies can be classified into three main categories: solar electric, thermal and combined power / cooling [8]. Some of them are already available in the markets with much cheaper prices.

In recent decades, several researchers attracted by solar cooling since the heat necessary for the operation of the refrigerating machine is supplied by the sun, so the cold supplied is free. Like the summaries of a few subsequent articles, most of these articles focus on solar thermal cooling technologies. Ayman et al. [8] In this article, they examine and analyze different solar cooling technologies that can be used to provide the required cooling and refrigeration effect from solar energy. They have demonstrated that solar cooling is a clean and cost-effective technology, solar cooling offers environmental benefits, including reducing the demand from the main grid and shifting the load during peak usage and reducing gas emissions at greenhouse effect. DS Kim et al. [9], in this article they presented on the different technologies available to provide refrigeration from solar energy. They made a comparison between the different solutions both from the point of view of energy efficiency and economic feasibility. Solar electric and thermomechanical systems appear to be more expensive than thermal sorption systems. In terms of performance the absorption and adsorption system are comparable, but adsorption coolers are more expensive and bulkier than absorption coolers. Agnimoan et al. [10] have made the bibliographical synthesis on Solar absorption air conditioning, operating mode and description of the different elements of a solar air conditioning unit in the world. This work describes the constituent elements of absorption solar air conditioning, the disadvantages and advantages of this system. Monne et al. [11] carried out a study on the stationary analysis of a solar absorption LiBreH2O refrigeration system. This work describes the operation of this system. Their results show that the coefficient of performance (COP) reached values greater than 0.5 for the average cooling capacity between 3.6 kW and 5.8kW. Assilzadeh et al. [12] carried out the study on the Simulation and optimization of a solar absorption cooling system Lithium Bromide (LiBr) with evacuated tube collectors. Their experimental results show that the demand for cooling is high during periods when solar radiation is high. They studied the case of the Malaysian climate. Maher et al.[13] carried out the study on the optimization of solar cooling system. This work deals with the performance of the solar absorption cycle by varying the temperatures of the components. The value of COP is optimized to 0.776 for the values of generator 55 to 85 ° C, condenser and absorber is 30 ° C of evaporator 10 ° C. Olivier et al. [14] carried out the study on the Modeling and experimental validation of the solar loop for absorption solar cooling system using double glazing. This work estimates the capacity and performance of this system in relation to external factors. Their experimental results show that the performance of this system is linked to its heat source. Syed et al.[15] made study on A new experimental study of a solar cooling system in Madrid. This work presents the experimental results of this system in Madrid Spain. Their results show that the maximum COP is 0.6. Riffat et al. [16] explained the principle of thermoelectric operation and the materials used for the thermoelectric and its application. They also discussed the application of thermoelectric devices in refrigeration and power generation, and as a sensor of thermal energy, they discussedthe development of new materials that could improve thermoelectric devices for many applications. Noël Djonyang et al[17]have shown that the production of cold from this energy source is possible. Solar air conditioning could therefore be a relevant solution to produce renewable solar cooling. Solar cooling can be broadly classified into solar electric refrigeration, solar thermal refrigeration and solar thermal air conditioning. Klein and Reindl[18] studied the electrical characteristics produced from photovoltaic cells and compared them to the required characteristics of the compressor motor. Riffat et al [19] carried out a comparative study of the performances between the vapor compression cycle, the absorption cycle and the thermoelectric refrigerator. The comparison showed that vapor compression has a high COP and a low cost. However, some of the refrigerant vapor compression systems used will be phased out due to their effect on ozone depletion, such as the used R-12 or R-22 system. Mehmet et al [20] studied the possibility of improving thermal comfort in the habitat of the city of Adana, Turkey, through the use of the

solar electric vapor compression refrigeration system (SE-VCR) for different evaporation temperatures. It has shown that the SE-VCR system can be effectively used for daytime home cooling in the southern region of Turkey. Noël Ngueche et al. [21] contribute to improving the thermal comfort of living environments by using a cooling system coupled with an SE-VCR solar installation for the city of Maroua in Cameroon. They have shown that the proposed SE-VCR system can be used successfully in dry tropical areas to improve thermal comfort.

Several studies have been carried out in the field of solar technology, among these different systems, the vapor compression machine coupled to solar panels seems very promising in the air conditioning of housing [22]. The biggest advantage of using solar panels for refrigeration is the simple construction and high overall efficiency when combined with a conventional vapor compression system [9]. During the hot period, the energy consumption in the building is greatly increased, due to the use of traditional air conditioning systems. Research on the evaluation of the performance of solar electric vapor compression refrigeration system in Madagascar is still non-existent. Madagascar one of the countries with the largest solar deposit the world. Indeed, the duration of sunshine or insolation can reach of approximately 2,800 hours per year in all regions. However, the country has an enormous potential in solar energy, estimated 2000kWh / m^2. year for the regions in the center of the island and in the East and can reach 2168 kWh / m^2. year in some northern and southwestern regions. This potential is still little exploited for electricity production, solar heating, refrigeration and air conditioning. During the decade, the idea of harnessing the heat generated by photovoltaic modules attracted the attention of several countries in the world. The use of solar energy in combination with air conditioning systems powered by electricity or heat can represent a solution to reduce the electricity consumption of this sector.

The objective of this research is to contribute to the improvement and development of a solar vapor compression refrigeration system in a residential building in Madagascar to ensure thermal comfort and to evaluate its performance. To achieve our goal, it is important to note that a building of the same constructive design was used in the 5 cities, which are located in different climatic zones. First, the hourly cooling load capacities of a sample building during the months of January through May and October and December were determined using meteorological data such as hourly average solar radiation and atmospheric temperatures. Then, the variations of various parameters such as coefficient of performance, condenser capacity and compressor power consumption during the day were calculated for different evaporating temperatures. In addition, the minimum area of the photovoltaic panels has been determined to meet the compressor power demand according to the hourly average solar radiation data. After determining the required surface area of the photovoltaic panels,

2. Presentation of the study area

Madagascar, is located in the Indian Ocean and geographically attached to the African continent, from which it is separated by the Mozambique Channel. It is the fifth largest island in the world after Australia, Greenland, New Guinea and Borneo. It is 1,580 km long, 580 km wide, and has an area of 587,000 km ^{2}. It is divided into six historic provinces such as: Antananarivo, Antsiranana, Fianarantsoa, Mahajanga, Toamasina and Toliara. Its capital is Antananarivo.

Table 1 Geographical situation and meteorological data

				Temp ° C		**Sunshine W / m²**		**Wind speed m / s**		
City	**Latitude**	**Longitude**	**Altitude**	**Max**	**Min**	**Max**	**Min**	**Max**	**Min**	**Type of climate**
Antsiranana	12 ° 16 ′ 58 ″ S,	49 ° 17 ′ 33 ″ E	6	34.7	16.4	1164	0	23.6	0	Tropical climate of transition
Mahajanga	15 ° 43 ′ 00 ″ S,	46 ° 19 ′ 00 ″ E	20	36.6	15.7	1167	0	12.1	0	Hot tropical climate
Toliara	23 ° 21 ′ 13 ″ S	43 ° 40 ′ 34 ″ E	8	34.2	12.9	1171	0	15.8	0	Subdesert tropical climate
Tamatave	18 ° 08 ′ 50 ″ S	49 ° 23 ′ 43 ″ E	10	34.3	14.2	1228	0	10.5	0	Humid tropical climate
Antananarivo	18 ° 54 ′ 44 ″ S	47 ° 31 ′ 18 ″ E	1276	31.7	3.9	1344	0	11	0	Tropical climate Altitude

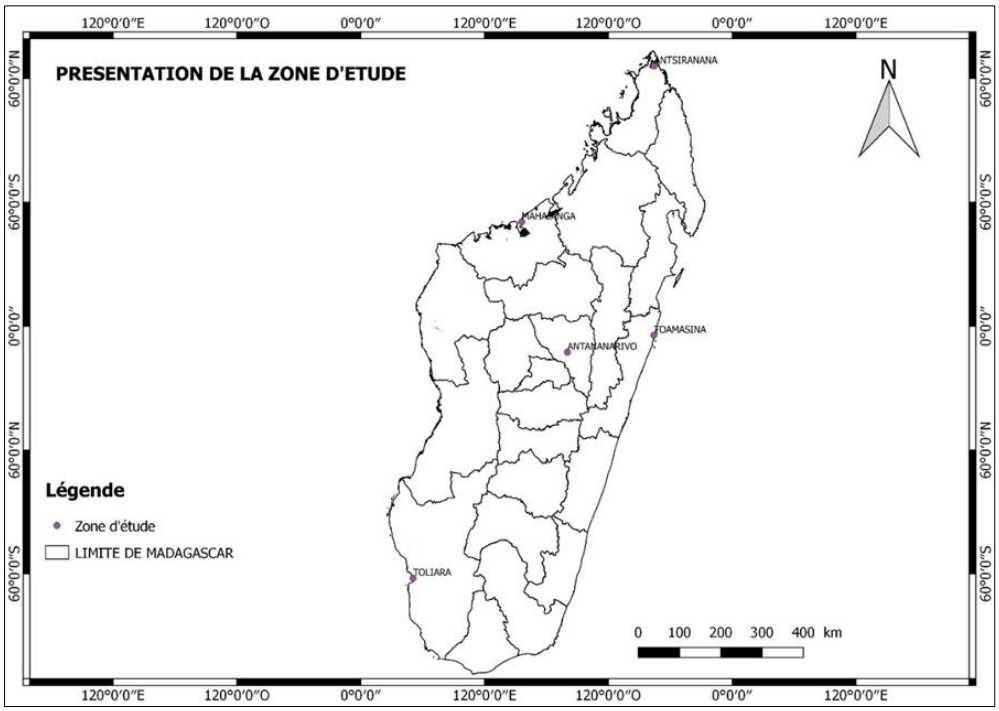

Figure 1 Presentation of the study area

3. Material and methods

In this study, we will evaluate the performance of an electric vapor compression solar refrigeration system. in different cities of Madagascar using the most recent hourly climate data for each selected city such as outdoor air temperature, relative humidity, and sunshine.In order to be able to analyze the performance of this system, it is important to note that a building of the same constructive design was used in the selected cities, which are located in different climatic zones.

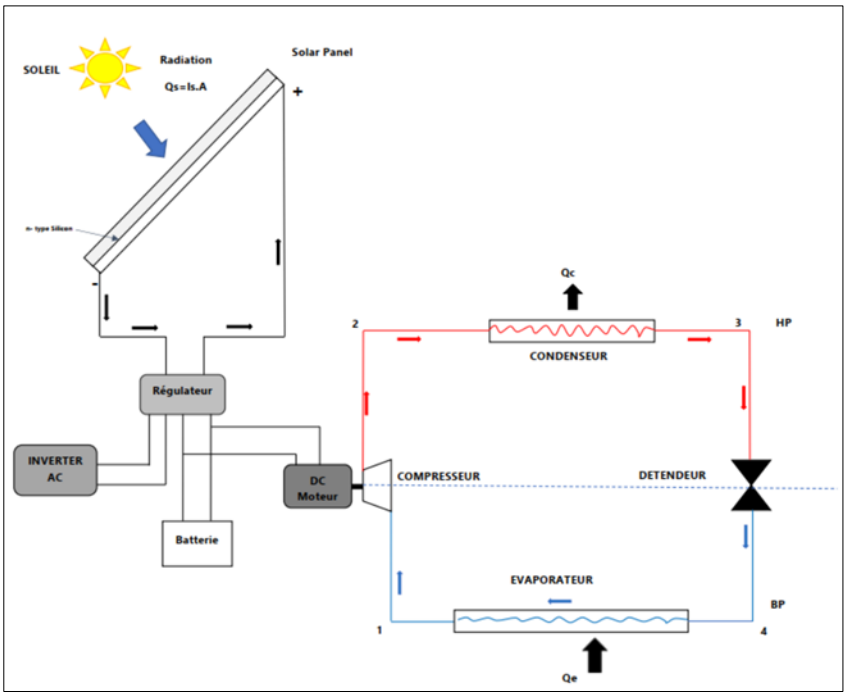

Figure 2 Diagrams of the operating principle of the SE-VCR system

The descriptive diagram of an electric vapor compression solar refrigeration system is shown in Figure 2 above. As shown in this figure, the SE-VCR system mainly consists of photovoltaic panels, a DC motor, a compressor, a condenser, an evaporator, an expansion valve, batteries, an inverter and a charge controller. This system uses an electric motor that works with solar energy. This motor is used to drive the compressor for a conventional air conditioning system. The batteries are used to store the excess energy produced by the solar panels throughout the day and keep this system running at night. The motor consumes the most energy in this system, the electrical energy demand of the motor is met both by the direct energy production of the solar panels and the batteries depending on the amount of solar energy throughout the day. The regulator protects the batteries in the event of overloads and deep discharges.

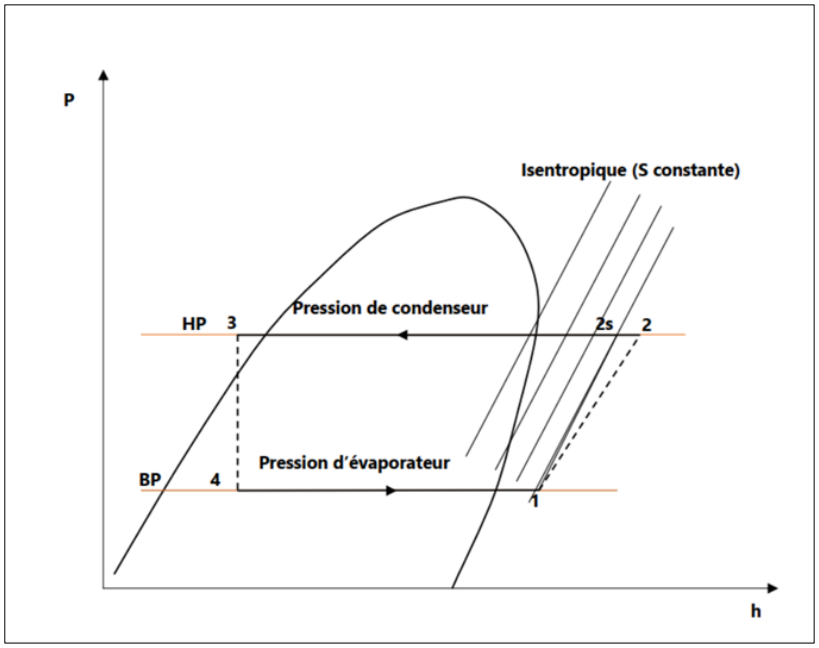

Figure 3 Representation of the operating point of the system on the (h-p) diagram

The SE-VCR system assumptions are as follows:

The refrigerant used for the vapor compression refrigeration cycle is R717 refrigerant or NH3 ammonia. Saturated vapor enters the compressor and saturated liquid leaves the condenser. The compressor and the expansion valve operate adiabatically. The irreversibility between the evaporator and the condenser are neglected.

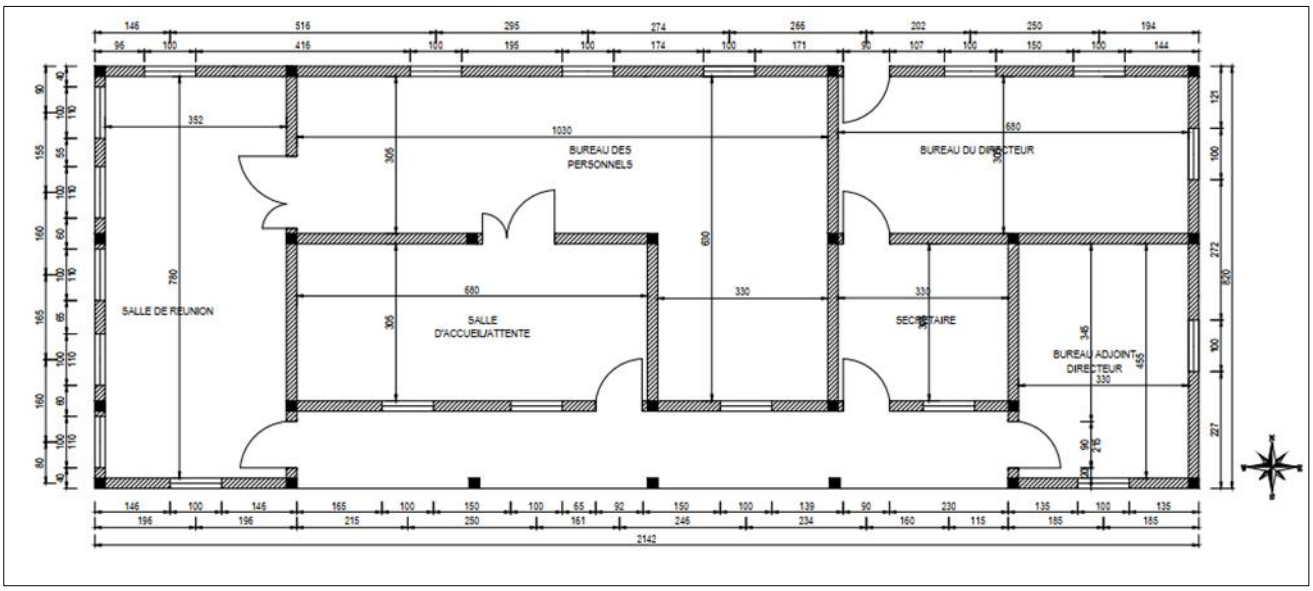

Figure 4 Plan view of the building to be studied

The construction elements of the walls of this building and their thermal characteristics are presented in the table below.

Table 2 Materials for wall construction and their thermal characteristics

Construction Materials	Thermal conductivity (W / m. K)	Thickness (m)
Exterior cement plaster	1.15	0.015
Cement block	0.952	0.2
Interior cement plaster	1.15	0.015

3.1. Hourly climate data

As part of this study, hourly climatic data for the city of Antsiranana, Mahajanga, Toliara, Antananarivo and Toamasina were downloaded with the more recent version of the Météonorm software. This tool has been used by many researchers because it is possible to have meteorological data for more than 2,100 meteorological sites around the world. For this software it is possible to have data such as the external time parameter of each city selected in the form of ".dat" files. It is a collaborative software that facilitates exports to TRNSYS from CSTB as well as many other simulation software in solar energy and building. It is aimed at engineers, architects, teachers, designers and anyone interested in solar energy and climatology.

3.2. Vapor Compression Refrigeration System Analysis

- The power indicated by the compressor is given by the following relation [21]:

$$Q_{cp} = \dot{m}(h_{2r} - h_1) = \dot{m}\frac{(h_{is} - h_1)}{\eta_{is}} \quad (1)$$

- The effective power on the compressor shaft is given by the following relation [21]:

$$Q_{eff} = \dot{m}\frac{(h_{is} - h_1)}{\eta_{is}.\eta_m} \quad (2)$$

With $\dot{m}$ refrigerant mass flow rate, h_i mass enthalpy for the transformation to state i, η_{is} and η_m are the isentropic efficiency and the mechanical efficiency of the compressor, respectively.

- The condenser power is [21]:

$$Q_c = \dot{m}(h_{2r} - h_3) \quad (3)$$

- The isentropic efficiency is given by the following relation [21]:

$$\eta_{is} = \frac{h_{is} - h_1}{h_{2r} - h_1} \quad (4)$$

$$\eta_{is} = 0.874 - 0.0135x\frac{P_c}{P_e} \quad (5)$$

- The evaporator power is written [21]:

$$Q_{ev} = \dot{m}(h_1 - h_4) \quad (6)$$

- The system balance can be written as follows:

$$Q_c = Q_{ev} + Q_{eff} \quad (7)$$

- The mass flow rate and the volumetric efficiency are given by the following relation [21]:

$$\dot{m} = \frac{\dot{V}_b}{V_1}\eta_v \quad (8) \text{ and } \eta_v = \frac{\dot{V}_a}{\dot{V}_b} \quad (9) \text{ with } \dot{V}_b = \frac{\pi \dot{D}^2 ZNL}{4x60} \quad (10) \text{ and } \dot{V}_a = \dot{m}\nu_1 \quad (11)$$

With $\dot{V}_a$ volume flow at the compressor inlet and $\dot{V}_b$ volume swept per unit time of the compressor, nc number of pistons, N number of rotations (rev / s), L piston stroke of the piston and D piston diameter.

- Coefficient of performance of the refrigeration cycle:

It is obtained by the following relation [21]:

$$COP = \frac{Q_{ev}}{Q_{eff}} = \frac{(h_1 - h_4)}{(h_{2is} - h_1)}.\eta_m \quad (12)$$

- Refrigeration cycle efficiency:

It is given by the following relation [21]:

$$\varepsilon = COP\left(\frac{T_c - T_{ev}}{T_{ev}}\right) = \frac{(h_1 - h_4)}{(h_{2is} - h_1)}.\eta_m\left(\frac{T_c - T_{ev}}{T_{ev}}\right) \quad (13)$$

With TE and TC being respectively the evaporation and condensation temperatures of the cycle considered.

- Coefficient of performance of the heat cycle:

It is obtained by the following relation [21]:

$$COPcal = \frac{Q_{con}}{Q_{eff}} = \frac{(h_2 - h_3)}{(h_{2is} - h_1)}.\eta_m \quad (14)$$

- Heat cycle efficiency:

It is given by the following relation [21]

$$\varepsilon_{cal} = COPcal\left(\frac{T_c - T_{ev}}{T_{ev}}\right) = \frac{(h_2 - h_3)}{(h_{2is} - h_1)}.\eta_m\left(\frac{T_c - T_{ev}}{T_{ev}}\right) \quad (15)$$

3.3. Analysis of different thermal loads

- Thermal transmission through facades (walls, roof, ceiling and floor) and glazing

The heat transmission through facades and glazing is obtained by the following relation [21]:

$$Q_{paroi} = KS\Delta T \quad (16)$$

With K heat exchange coefficient, S: surface of the wall or window S (m^2), ΔT the difference between the outside and inside temperature.

- Heat input by solar radiation through the facade.

Heat transfer by solar radiation is obtained by the following relation [21]:

$$Q_{ray} = \alpha_p . F . S . R_m \quad (17)$$

From where α is the absorption coefficient of the wall receiving solar radiation, F factor of the solar radiation area, S the area of the walls S (m^2) and R_m solar radiation absorbed by the walls (W / m^2).

- Heat input by radiation on the glazing

It is given by the relation

$$Q_{ray} = \alpha_v . g_v . S . R_v \quad (18)$$

From where α is the absorption coefficient of the glazing, g reduction factor according to the type of window, S the surface of the walls S (m^2) and R_v solar radiation absorbed by windows (W / m^2).

- Heat input by air renewal and infiltration

There are two types of heat supply by air renewal and infiltration.

- The significant gains by air renewal given by the following relation:

$$Q_{sr} = q_v \left(T_e - T_i \right) x 0.33 \quad (19)$$

- Latent gains by air renewal obtained

$$Q_{Lr} = q_v \left(\omega_e - \omega_i \right) x 0.84 \quad (20)$$

Where qv is the air renewal rate (m3 / h), Te and Ti are respectively the outside and inside temperature, ω_e and ω_j are respectively the outdoor and indoor water content (g / kg dry air).

For natural ventilation, we can consider that the flow of fresh air is equal to the room volume per hour (1Vol / h).

- Heat input by occupants

There are two types of heat gain generated by occupants:

- ❖ Sensitive gains given by

$$Q_s = n . C_{soc} \quad (21)$$

- ❖ Latent gains given by occupants

$$Q_L = n . C_{Loc} \quad (22)$$

- Heat input by lighting

The heat input by lighting is a sensible heat source depends on the type of fluorescent lamp. It is evaluated using the following formula:

$$Q_{el} = 1.25P \quad (23)$$

For the incandescent lamp:

$$Q_{el} = P \quad (24)$$

- Heat input by machinery and equipment

Most devices are both a sensible and a latent heat source. The heat inputs by machines and equipment are determined from data provided by manufacturers. These machines and equipment must be multiplied by the coefficient a according to their operating times. For example, a device operating for half an hour releases half of its electrical heat input.

- Total thermal loads

The total heat balance (Q_T) is the sum of all internal and external loads. It is more practical to add sensitive loads Q_S and latent loads Q_S.

$$Q_T = Q_s + Q_L \quad (25)$$

- Total sensitive loads

These are the contributions of sensible heat in the room, due to the difference between indoor and outdoor temperatures.

$$Q_S = Q_s + Q_{sr} + Q_{equipement} + Q_{paroi} + Q_{soc} \quad (26)$$

- Total latent heats

These are the contributions of latent heat due to the difference in the amount of interior and exterior water vapor:

$$Q_L = Q_{Lr} + Q_{Loc} + Q_{equipement} \quad (27)$$

3.4. Solar photovoltaic production system analysis

Photovoltaic cells transform light into electricity by photoelectric effect. Photovoltaic cells made of semiconductor materials, monocrystalline thin films, polycrystalline wafers and silicon are the materials for solar panels, and silicon is a major component of photovoltaic cells in the market.

The following equation defines the efficiency of the solar panel, it is obtained by the peak power ratio W (kWp) to the product of its area Apv (m^2) and the direct solar irradiation in Is (kW / m^2) [9].

$$\eta_{pv} = \frac{W_{cr}}{I_s x A_{pv}} \quad (29)$$

The Peak Watt is a unit of the maximum power that a solar photovoltaic module can produce under optimal sunshine and temperature conditions. That is, when the instantaneous power of the sun is 1000 W / m^2 and the cells of the module are at a temperature of 25 degrees centigrade.

The efficiency of polycrystalline thin films is higher than that of silicon wafer, the efficiency of polycrystalline thin films in a range of 10-17% [7], the efficiency of monocrystalline thin files can reach 15-20% in using multi-junction cell structure, while silicon wafer performance is low and cost high.

The energies produced by solar panels should meet the energy needs of the compressor. The energy needs of the compressor during the whole day is obtained by the following relation [20]:

$$E_{cp} = \sum_{i=1}^{k} E_i \quad (k = 1 \text{ to } 24) \quad (30)$$

The amount of electrical energy produced by solar PV modules is directly proportional to the Sunshine of the site where the system. It is given by the following relation [12]:

$$E_{pv} = A_{pv} x \left(\sum_{i=1}^{k} I_i \right) \text{ (k = 1 to 24) (31)}$$

The peak power to be installed is obtained from [21]:

$$W_{cr} = \frac{E_c}{I_s x R_b x R_i} \text{ (32)}$$

With Rb and Ri are the energy efficiency of the batteries and the installation respectively.

$$Puissance\ crête = \frac{Daily\ energy\ requirement\ of\ the\ compressor\ (in\ kWh)}{Sunshine\ x\ correction\ factor} \text{ (32)}$$

This formula takes into account the energy losses in the various components of a PV system. Voltage drops in cables, the power drop caused by the elevation temperature of the module in operation, drops in voltage at the regulator and the uncertainty on the meteorological data are taken into account by the factor K = RbxRi.

The capacity C of the batteries is obtained from [21]:

$$C = \frac{Production\ d'énergie journalière x\ nombre\ de\ jour\ d'autonomie}{Daily\ energy\ production\ x\ number\ of\ days\ of\ autonomy} \text{ (33)}$$

The overall efficiency of the installation η_g is given by the following relation:

$$\eta_g = \frac{Q_T}{I_T x A_{pv}} \text{ (34)}$$

4. Results and discussion

4.1. The limits of this system

The main limitations of this system are: the very high purchase cost, this system requires a large surface for the installation of the panels and the batteries, the users require training for the operation of this system, the performance of this system. This system depends on compliance with operating instructions, quality and frequency of maintenance. The use of solar energy requires an investigation and research of meteorological data in the field to properly size this system on the place where it is to be installed. As already mentioned in section 3.1, this study is based on meteorological data obtained with the Meteonorm software. To validate these data, it is necessary to carry out measurements in the field in order to have reliable and concrete data.

4.2. Thermal load balance

The different heat transfers through the environment are given in the tables. For equipment, we have two photocopiers, twelve desktops, two laptops. The office accommodates 18 people.

Using a 5% increase coefficient, the overall heat balance will be equal to $Q_T = 1.05 * Q_t$

The thermal balance of this building varies as a function of time as shown in Figure 5 below.
Figure 5 shows the total heat loads in W for each selected city.

Table 3 Thermal characteristics of the building construction elements of walls, windows, doors, ceiling for the city of Mahajanga

Wall orientation	K (W / m². K)	Surface (m²)	Radiation Intensity (W / m²)
West wall	2.46	21.15	455
North wall	2.46	60,815	288
South walls	2.46	59.09	-
East wall	2.46	24.45	308
Roof ceiling	0.60	181,608	500
Single pane window East	6.15	2.2	400
South single glazed hinged door	6.15	8.8	-
North single glazed hinged door	6.15	2.2	300
Single glazed window South	6.05	6.6	300
Single glazed window North	6.05	6.6	300
West single glazed window	6.05	5.5	455

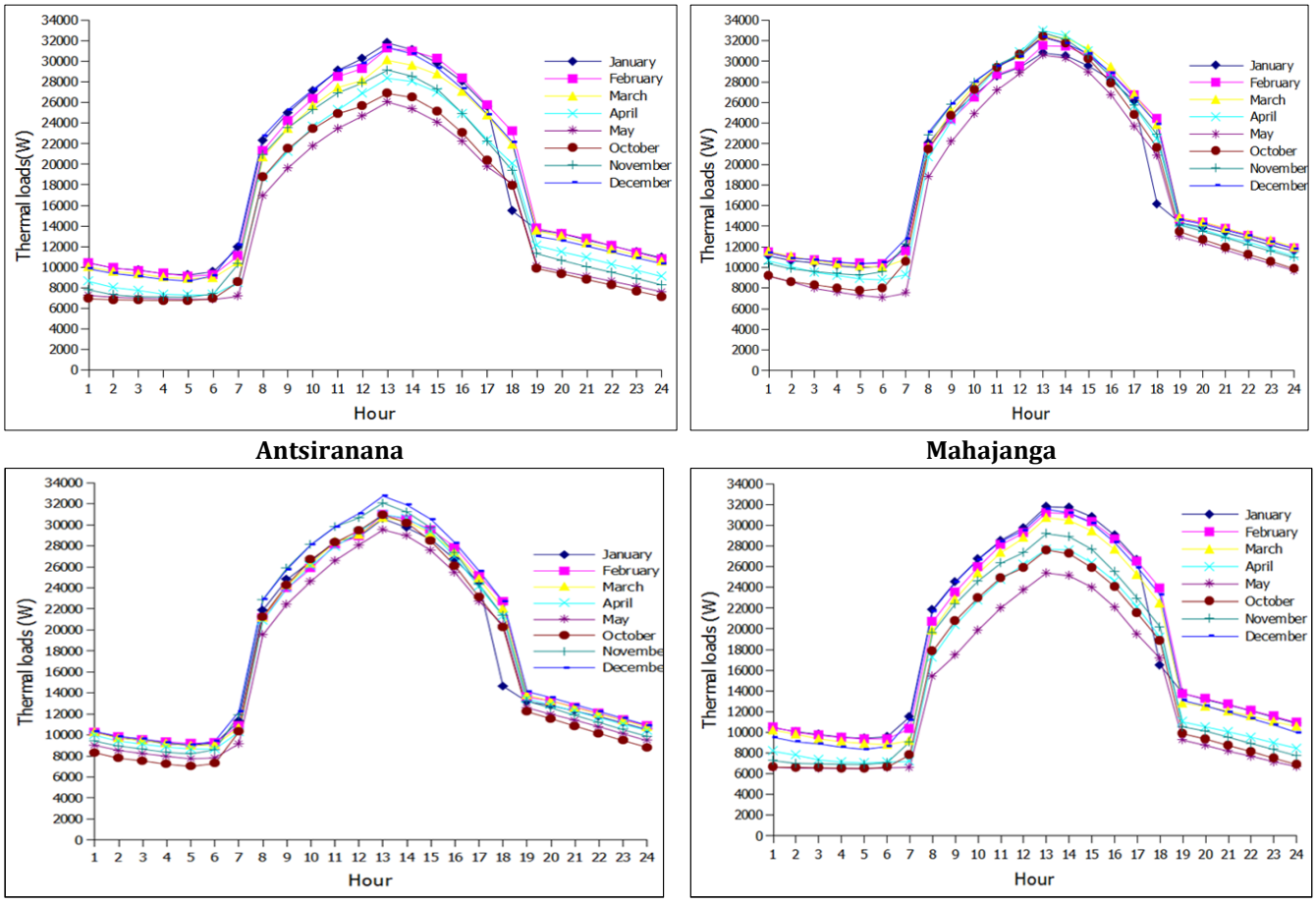

Figure 5 Hourly variation of the thermal loads of the building from the 1 day of the month January to December

Figure 5 shows the hourly variations in total heat loads in W for the month of January-May and in the month of October to December for the 4 selected cities. In the 4 figures, we have seen that the charge is maximum around 1 p.m. while the minimum is at 6 a.m. For the case of Antsiranana and Toliara the maximum thermal loads occur in the month of January with a respective value of 31.78 kW and 31.80 kW, for the city of Mahajanga, they occur in the month of April with a value of 32.97 kW and in the month of December for the city of Tamatave with a value of 32.73 kW. The results of these 4 cities show that the maximum thermal loads have a small difference from each other, as for example for the city of Mahajanga and that of Toliara has a load difference of 1.69 kW and 0.95 that of Tamatave and Antsiranana. For these 4 cities, Mahajanga presents a maximum thermal load compared to the other cities. The thermal loads vary less with respect to each other in the month of January to December. The outdoor temperatures and sunshine during these months vary less, which explains the variation in these thermal loads. In May, the thermal load is low, this decrease is due to the decrease in the outside temperature. In general, thermal loads are higher from9 a.m. to 5 p.m. and lower 6 p.m. to 6 a.m. It is also noted that the period of high thermal loads corresponds to high activities in the building, which results in the need for the reduction of the interior temperature in the building. Noel Djongyang et al[17] found a maximum load of 22.89 kW in May. From June to September, the thermal loads are low and vary less with respect to each other for the city of Maroua. These two results (our results and the results of Noel Djongyang et al[18] for the city of Maroua) are very different. They are very different since the dimension of the building to be studied is not the same and the different internal loads also, we used a building of dimension (8.20x21.42) while they used (13x5), we have a number 18 occupants while they have only 13 occupants and the number of equipment to use.

Table 4 Thermal loads due to occupants, equipment and air renewal for the city of Mahajanga

Thermal loads	Heat sensitive W	Latent heat W	Total [W]
Air renewal	927.72	3160.9	4089
Occupants	71.8	60.1	131.9
Equipment's	9831	-	9831

4.3. Calculation of the compressor power consumption

Knowing all the characteristics of the operating points of the SE-VCR system on the enthalpy diagram (Ph NH3), figure 6 below shows the hourly variation in the electrical consumption of the compressor for an evaporating temperature of 0 ºC and a temperature of condensation of 40 ºC on the 1st day of the months from January to December at 1 am. FIG. 4 shows the hourly variation in the electrical consumption of the compressor accumulated over 24 hours.

Table 3 Characteristics of the installation's operating points on the (h-p) NH3 diagram for an evaporation temperature of 0 ° C

Points	1	2s	2	3	4
Temperature ° C	0	92	107	40	0
Pressure in bar	4.375	15.6	15.6	15.6	4.375
Enthalpy kJ / kg	1763.637	1945.45	1983.78614	690,909	690,909

Table 4 Monthly variation of the effective compressor power for each city selected

City	Powers	Jan	Feb	Mar	Apr	May	Oct	Nov	Dec
Antsiranana	Pcp (kW)	7.67	7.55	7.26	6.84	6.29	6.48	7.04	7.56
Mahajanga	Pcp (kW)	7.44	7.61	7.83	7.96	7.38	7.82	7.91	7.8
Toliara	Pcp (kW)	7.68	7.54	7.42	6.68	6.13	6.66	7.04	7.61
Tamatave	Pcp (kW)	7.38	7.49	7.4	7.48	7.13	7.47	7.74	7.9

Table 5 Monthly variation of refrigerant flow rates for each selected city

City	Mass flow rates	January	February	March	April	May	October	November	December
Antsiranana	kg / s	0.0296	0.0291	0.028	0.0264	0.0243	0.0251	0.0272	0.029
Mahajanga	kg / s	0.0287	0.0294	0.0302	0.0307	0.0285	0.0302	0.0306	0.03
Toliara	kg / s	0.0296	0.0291	0.0287	0.0258	0.0237	0.0257	0.0272	0.029
Tamatave	kg / s	0.0285	0.0289	0.0286	0.0289	0.0275	0.0289	0.0299	0.031

The maximum values are obtained between 9 a.m. to 5 p.m. with a maximum value of 7.96 kW in April at 1 p.m. and lower in May at 6 a.m. with a value of 1.7 kW.

(Noel Djongyang et al), found a compressor power varying from 5.33 to 6 kW. It is known that the power of the compressor varies according to the refrigerating capacity of the building, the more the refrigerating capacity increases the capacity of the compressor increases.

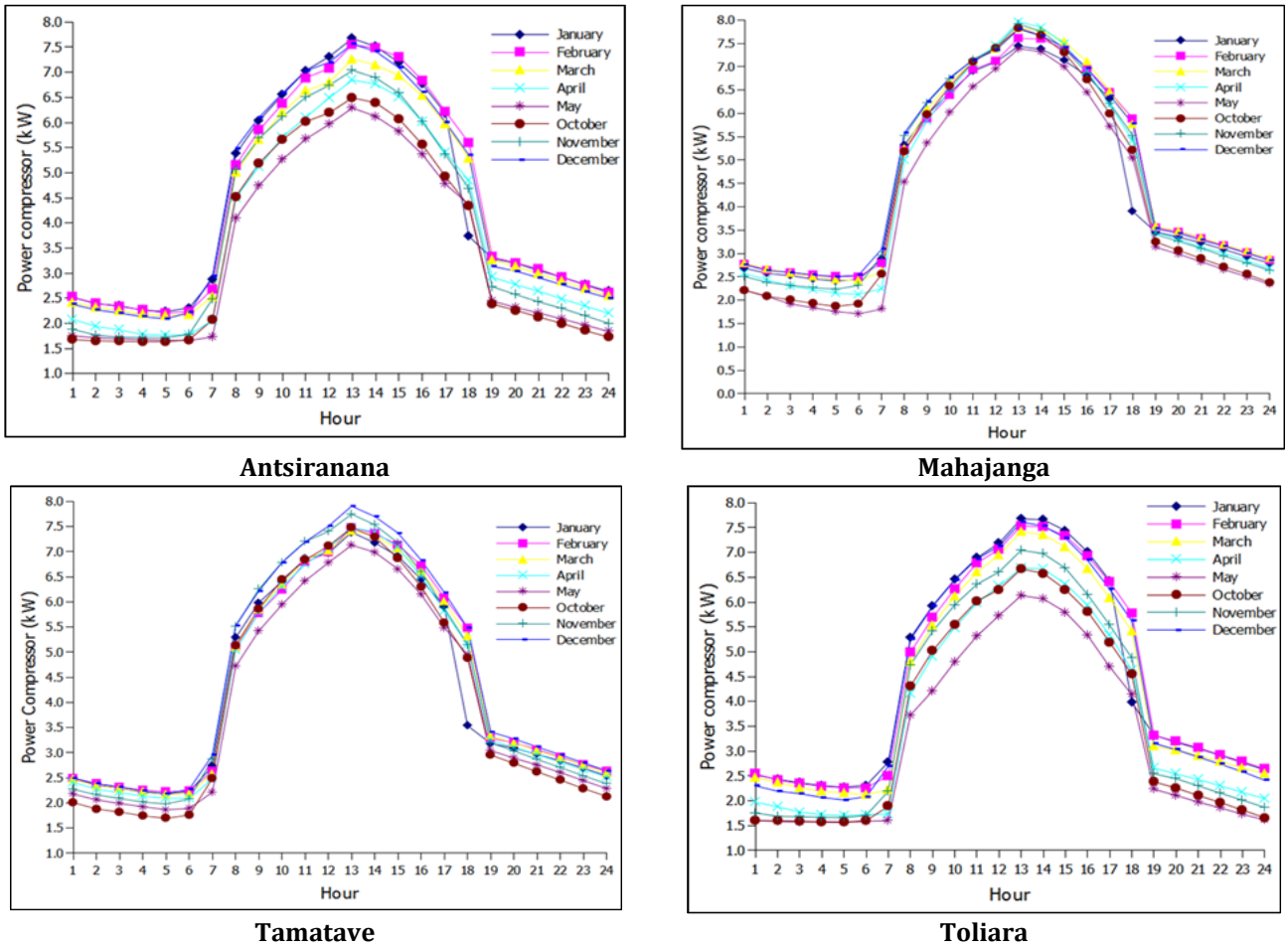

Figure 4 Hourly variation of the electrical consumption of the compressor for the 1st day from January to December for an evaporation temperature Te = 0 ° C

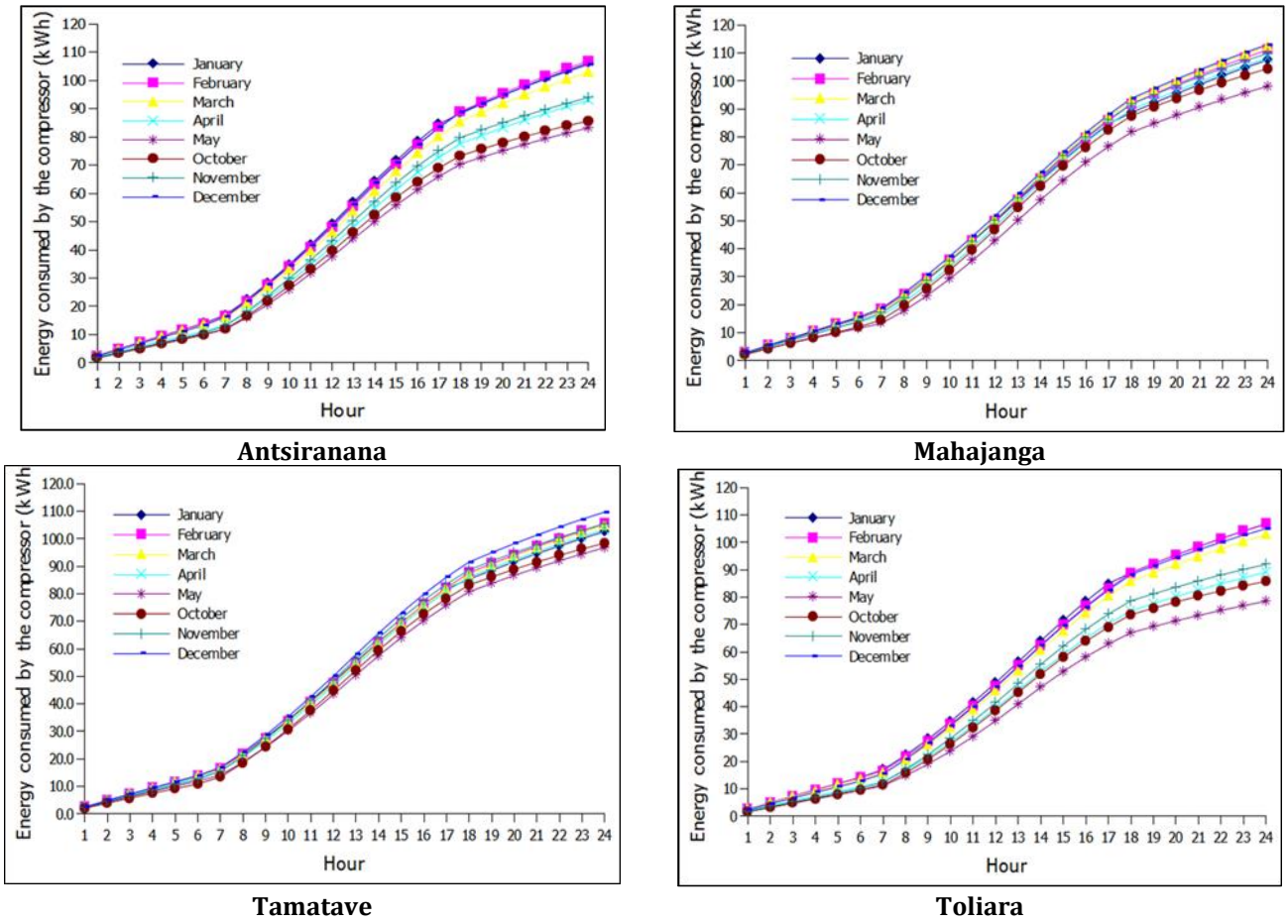

Figure 5 Hourly variation of cumulative electrical consumption of the compressor for an evaporating temperature of 0 ° C for each selected city

Table 8 Monthly variation of the SE-VCR system coefficient for an evaporation temperature Te = 0 ° C for the selected cities.

City	COP	Jan	Feb	Mar	Apr	May	Oct	Nov	Dec
Antsiranana	[-]	4.14	4.07	3.92	3.69	3.39	3.5	3.8	4.08
Mahajanga	[-]	4.14	4.24	4.36	4.43	4.11	4.36	4.43	4.34
Toliara	[-]	4.14	4.07	4	3.6	3.31	3.6	3.8	4.11
Tamatave	[-]	4.14	4.2	4.15	4.2	4	4.19	4.34	4.43

Figure 8 shows the variation of the hourly power consumption of the compressor for the evaporating temperatures of -10 ° C, -5 ° C, 0 ° C, 5 ° C and 10 ° C for the selected cities. From this figure, it has been observed that the power decreases with increasing evaporation temperatures. As for example in the case of the city of Mahajanga, for an evaporation temperature Te = 10 ° C, the compressor power varies from 1.52 to 5.24 kW around 1 a.m. to 1 p.m., while for Te = -10 ° C, the power varies from 3.2 to 10.8 kW. This figure shows the evaporating temperature has a significant influence on the compressor power.

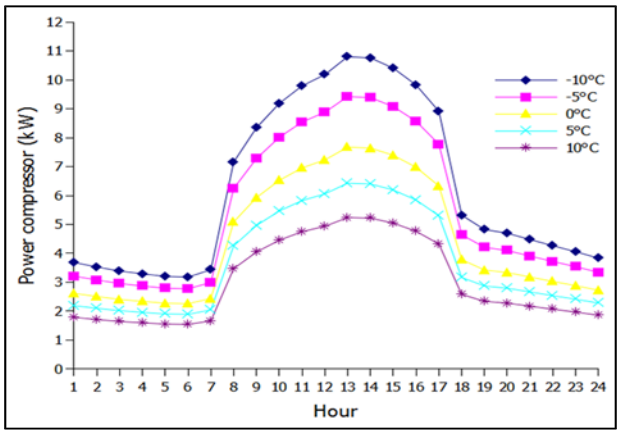

Antsiranana

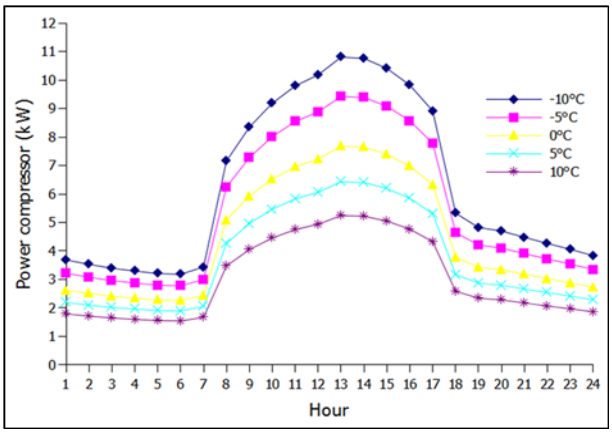

Mahajanga

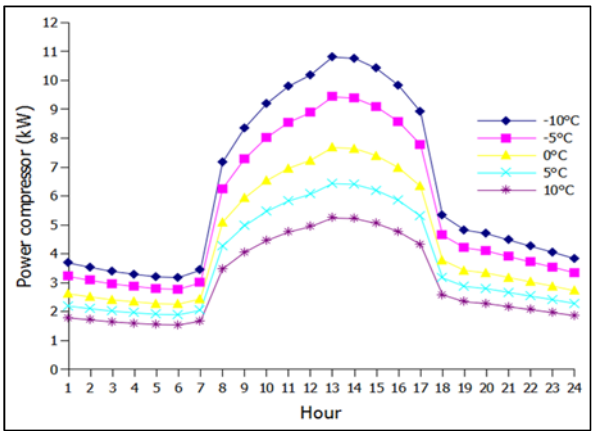

Tamatave

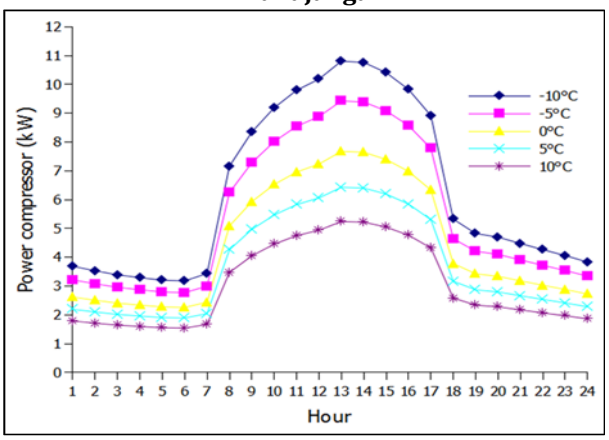

Toliara

Figure 6 Compressor power hourly variation for a 0 ° C, -10 ° C, 10 ° C, -5 ° C, 5 ° C and 10 ° C evaporating temperature variation for each city selected

4.4. Calculation of the coefficient of performance COP

The monthly change in coefficient of performance of SE-VCR system is shown in Table 7, and Figure 5 shows the hourly change for evaporating temperature at 0 ° C.

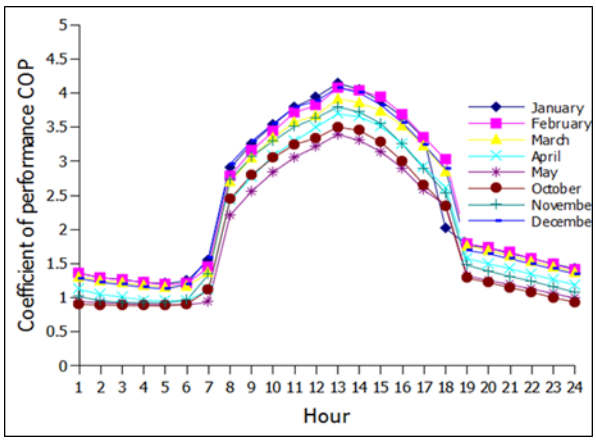

Antsiranana

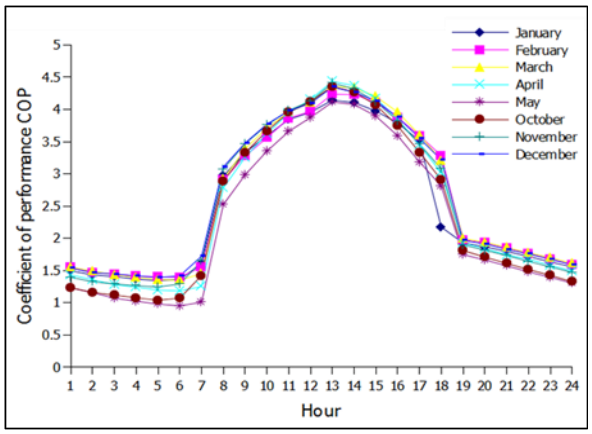

Mahajanga

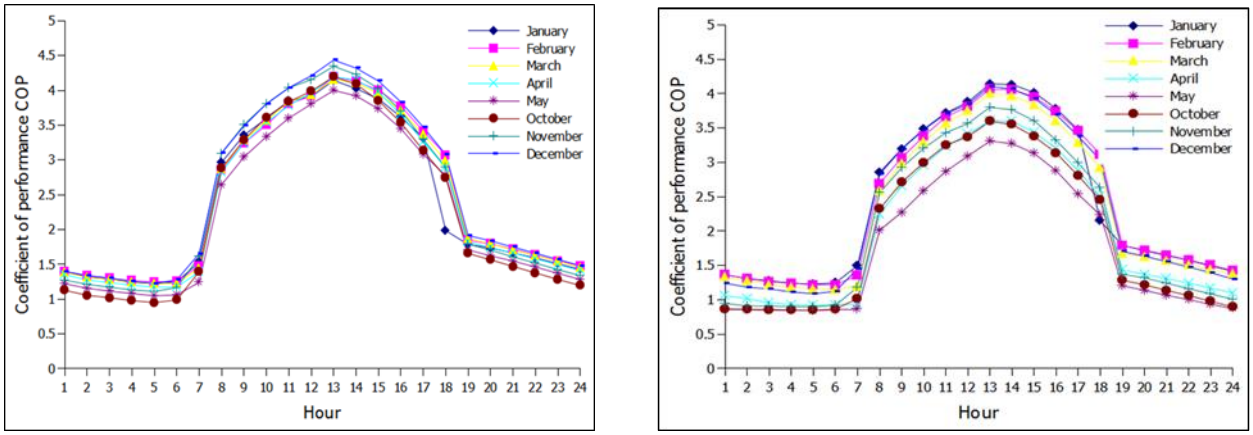

Figure 7 Hourly variation of the coefficient of performance for an evaporation temperature Te = 0 ° C

As shown in figure 9, this coefficient was calculated by evaluating atmospheric temperatures and heat loads for different hours of the day. In this figure, we see that the COP is lower at 4 to 6 a.m. with values between 1.36 and 1.40. This can be explained that at this time, the thermal load decreases significantly in the building which is caused by the absence of occupants and the decrease in atmospheric temperature. The highest values are obtained from 9 a.m. to 5 p.m. with values between 3.32 and 4.40. The maximum value is obtained in April around 1 p.m. with a value of 4.43 for the case of Mahajanga city. Regulations for new air conditioning installations require a COP value of at least 3 [22];

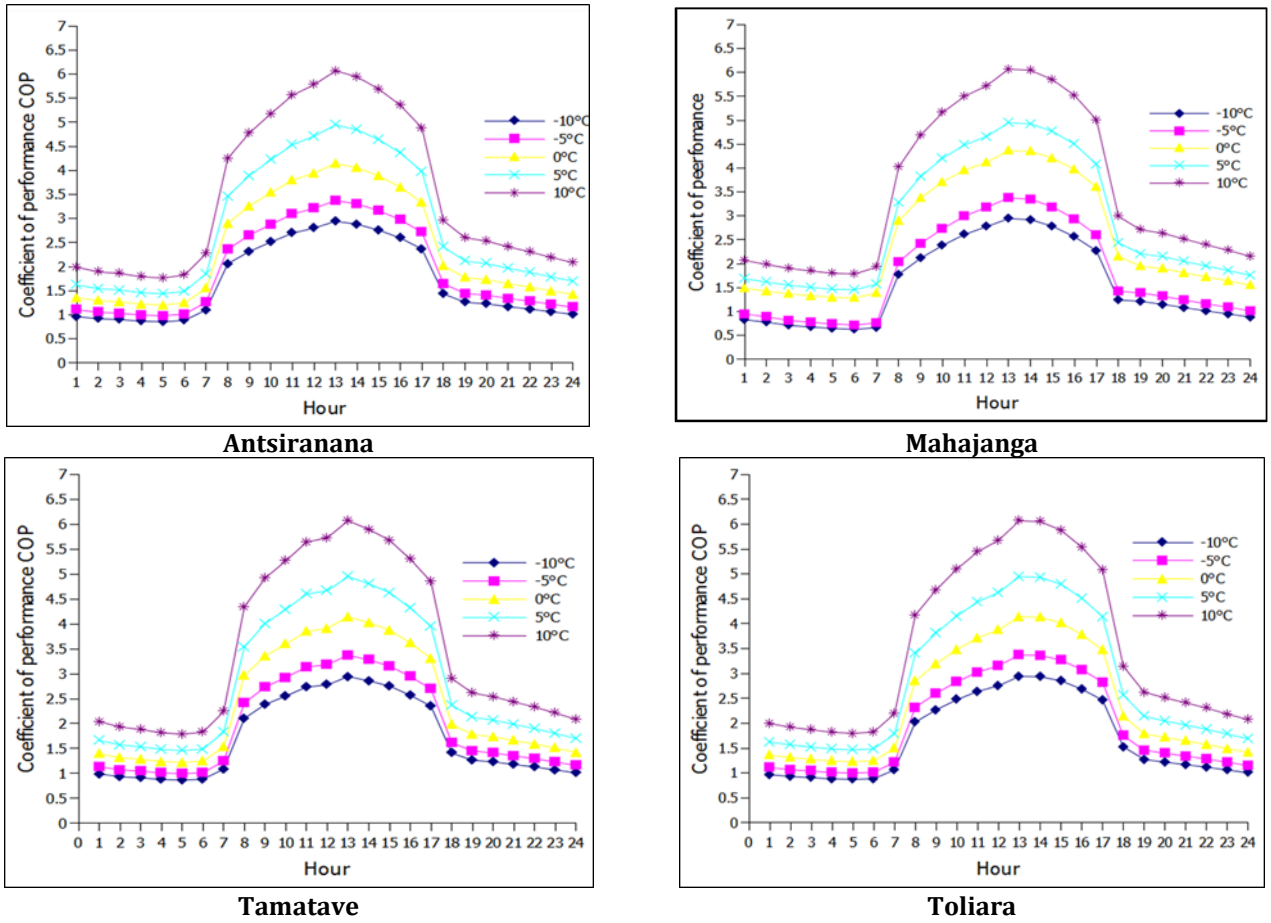

Figure 8 Hourly variation of coefficient of performance for a variation of evaporating temperature 0 ° C, -10 ° C, 10 ° C, -5 ° C, 5 ° C and 10 ° C for the first day of March for each city selected

Figure 10 shows the variation of the COP as a function of the evaporation temperature. In this figure, it can be seen that the evaporation temperature has a considerable influence on the coefficient of performance of this system. With an evaporation temperature of 0 ° C, the maximum COP coefficient varies from around 3.32 to 4.40 while it is slightly higher for an evaporation temperature of 10 ° C or it reaches a maximum value between 4.87 to 6.067. On the other hand, for an evaporation temperature of -10 ° C, it is of the order of 2.3 to 2.80.

4.5. Evaluating the condenser capacity

With an evaporating temperature of 0 ºC and a condensing temperature of 40 ºC, the condenser capacity values are shown in table 8.

The heat output of the condenser is also a function of the local heat load and the evaporating temperature, as shown in figure 11 below.

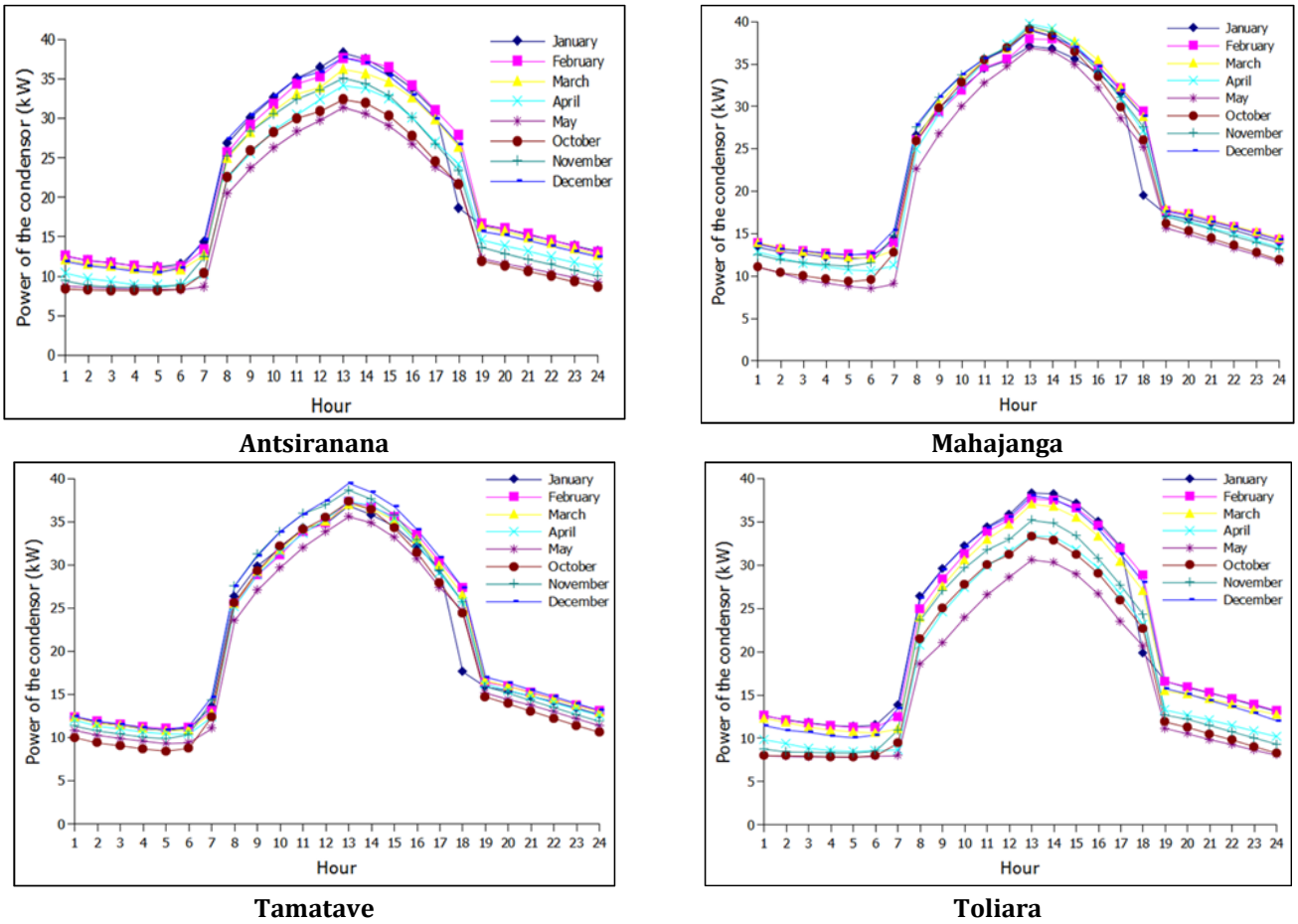

Figure 9 Hourly variation of the condenser power for an evaporation temperature Te = 0 ° C for selected cities

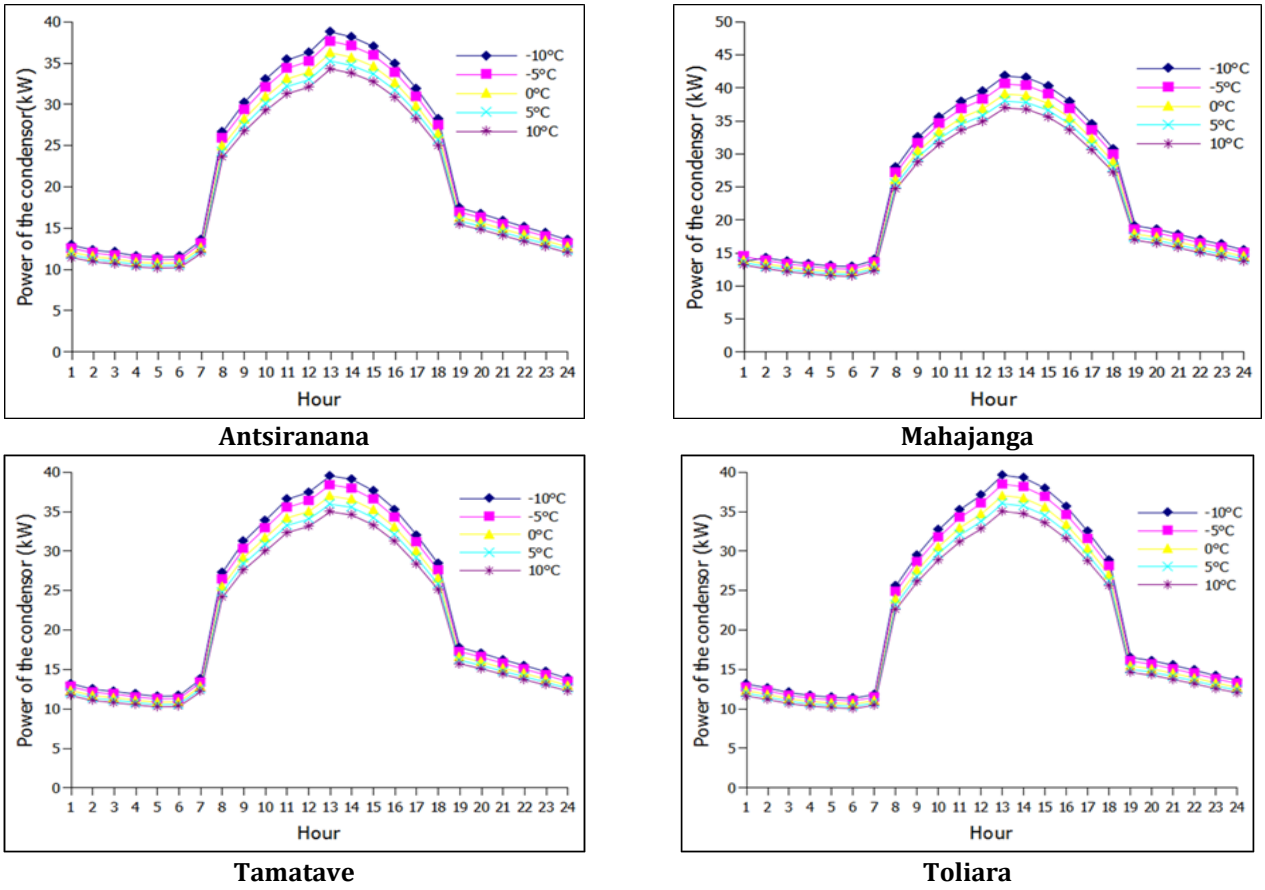

Figure 10 Hourly condenser variation for a 0 ° C, -10 ° C, 10 ° C, -5 ° C, 5 ° C and 10 ° C evaporating temperature variation for the first day of March for the selected cities

Table 6 Monthly variation of condenser power for an evaporation temperature of 0 ° C

City	Powers	Jan	Feb	Mar	Apr	May	Oct	Nov	Dec
Antsiranana	(kW)	38,306	37.68	36.25	34.17	31.39	32.4	35.13	37.75
Mahajanga	(kW)	37.12	37.97	39,064	39.73	36.86	38,248	39.04	39.96
Toliara	(kW)	38.33	37.63	37.04	33.36	30.6	33.27	35.16	38
Tamatave	(kW)	36.86	37.37	36.97	37.33	35.58	37.31	38.66	39.46

4.6. Power of the solar modules

For continuous use of the SE-VCR system, a battery with a capacity of 6000Ah was used, with an operating voltage of 48V and a discharge coefficient of 0.75 for an autonomy of two days. The batteries are used to store the excess energy produced by the solar panel for the whole day, and used in times when the PV generator is not working. The peak power of a single photovoltaic generator used is 400Wp and a supply voltage of 24V. The PV yield used is 0.2016. The panel area, installed power and number of installed panels for each selected city is shown in Table 9 below. It also presents the peak power to install panels.

Figure 13 Shows the hourly variation of the power produced by photovoltaic panels with the meteorological conditions of the cities selected for an evaporation temperature of 0 ° C.

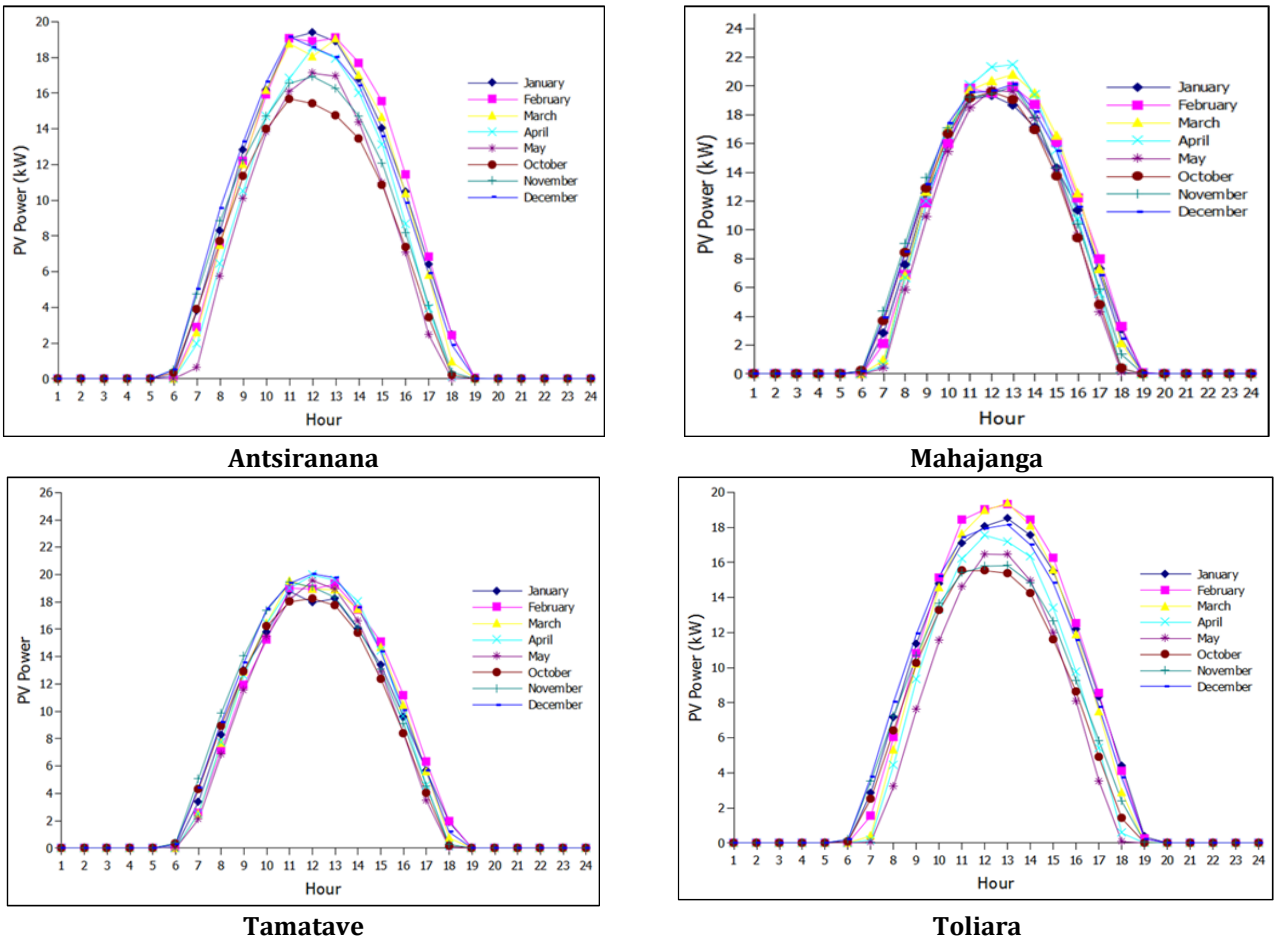

Figure 11 Hourly variation of the power produced by the PV for an evaporation temperature Te = 0 ° C for the selected cities

Table 7 PV sizing parameters for selected cities

City	Month	Jan	Feb	Mar	Apr	May	Oct	Nov	Dec
Antsiranana	Energy consumed kWh / day	106.1	106.8	102.9	92.9	83.2	85.7	93.9	105.6
	Sunshine KWh / m^2. Day	6.6	6.3	5.4	5.0	4.0	5.9	6.5	7.0
	Peak power to be installed (kWp)	22.2	23.4	26.4	26.1	28.9	20.1	20.0	21.0
	Number of panels to be installed	56.0	59.0	66.0	65.0	72.0	50.0	50.0	53.0
	Surface (m^2)	111.1	117.1	130.9	129.0	142.8	99.2	99.2	105.2
Mahajanga	Energy consumed kWh / day	107.4	111.1	112.5	108.1	98.1	104.4	109.8	113.0
	Sunshine KWh / m^2. Day	6.0	6.1	6.1	6.0	5.2	6.9	6.7	6.6
	Peak power to be installed (kWp)	25.0	25.2	25.6	24.9	26.1	21.2	22.9	23.8
	Number of panels to be installed	63.0	63.0	64.0	63.0	66.0	53.0	58.0	60.0
	Surface (m^2)	123.7	125.1	127.1	123.7	129.6	104.9	113.4	118.2
Tamatave	Energy consumed kWh / day	102.6	105.5	104.9	103.3	96.7	98.4	105.4	109.7
	Sunshine KWh / m^2. Day	6.0	6.2	5.9	6.0	5.2	6.7	7.0	7.0
	Peak power to be installed (kWp)	23.7	23.7	24.8	23.8	25.7	20.3	20.8	21.9

	Number of panels to be installed	59.0	59.0	62.0	60.0	64.0	51.0	52.0	55.0
	Surface (m^2)	117.1	117.1	123.0	119.0	127.0	101.2	103.2	109.1
Tamatave	Energy consumed kWh / day	102.6	105.5	104.9	103.3	96.7	98.4	105.4	109.7
	Sunshine KWh / m^2. Day	6.0	6.2	5.9	6.0	5.2	6.7	7.0	7.0
	Peak power to be installed (kWp)	23.7	23.7	24.8	23.8	25.7	20.3	20.8	21.9
	Number of panels to be installed	59.0	59.0	62.0	60.0	64.0	51.0	52.0	55.0
	Surface (m^2)	117.05	117,054	123.006	119,038	126.97	101.18	103.17	109.1
Toliara	Energy consumed kWh / day	106.72	106,793	102,822	89,089	78,479	85,752	91,944	105
	Sunshine KWh / m^2. Day	7,556	6.954	6.475	5.515	4,521	6.501	7,392	7.687
	Peak power to be installed (kWp)	19,618	21,328	22,055	22,435	24.11	18.319	17,275	18.97
	Number of panels to be installed	49	54	55	56	60	46	43	48
	Surface (m^2)	97,214	107,134	109,118	111,102	119.04	91,262	85.31	95.23

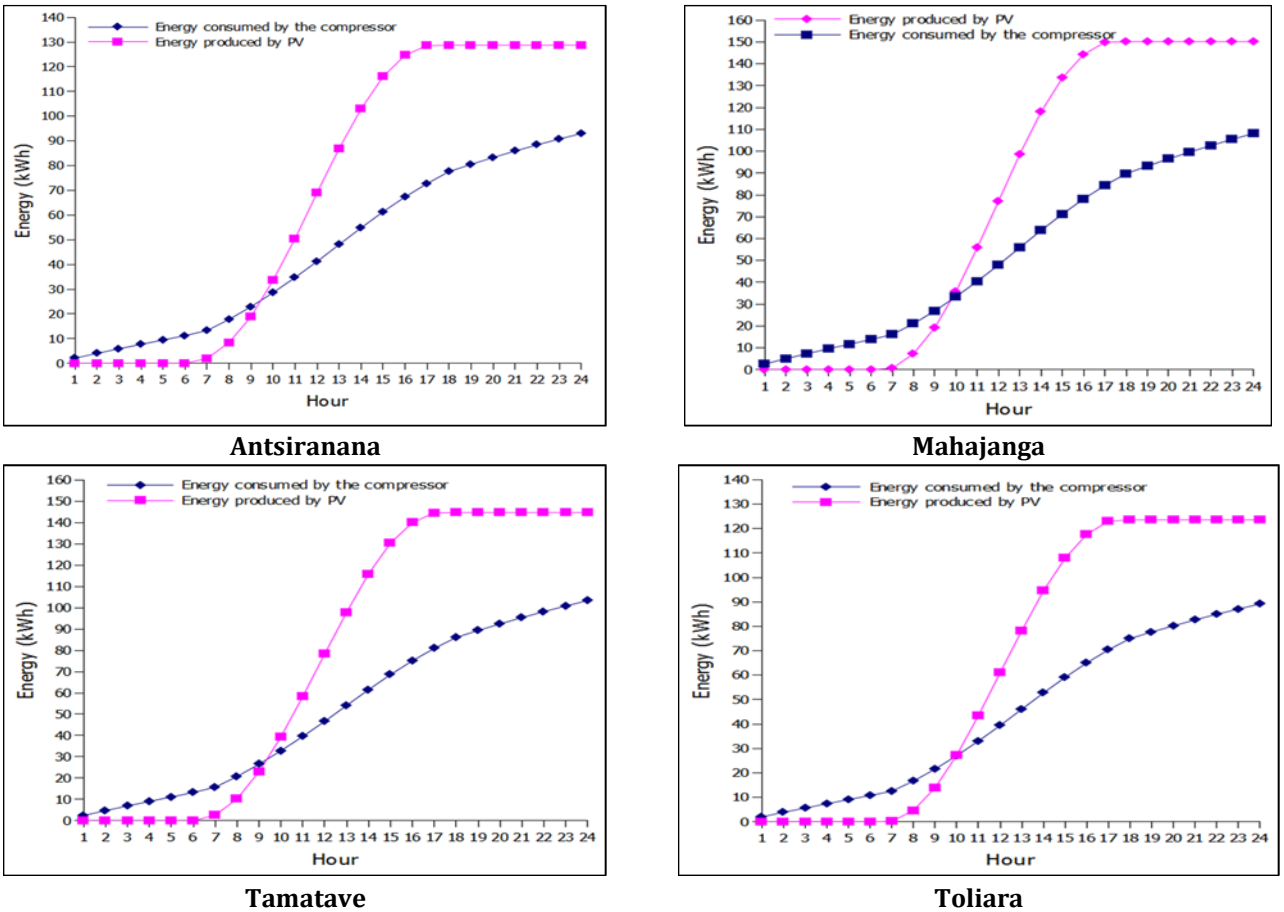

Figure 14 Comparison between the energy consumed by the compressor and the cumulative energy produced by the PV for temperature Te = 0 ° C in April for the selected cities

Figure 14 shows a comparison between the energy absorbed by the compressor and the energy produced by photovoltaic panels in April for an evaporation temperature of 0 ° C. It could be verified that between 10 a.m. and 6 p.m., the energy produced by the PV exceeds the energy consumption by the compressor. This excess energy could be stored in batteries for later use at low energy operating hours such as 7 p.m. to 6 a.m.

Figure 15 shows the hourly variation of the power of PV modules for evaporating temperatures of -10 ° C, -5 ° C, 0 ° C, 5 ° C and 10 ° C in March. It has been found to be low for an evaporation temperature of 10 ° C and higher for an evaporation temperature of -10 ° C. It could therefore be concluded that when the evaporating temperature decreases as the power of PV modules increase.

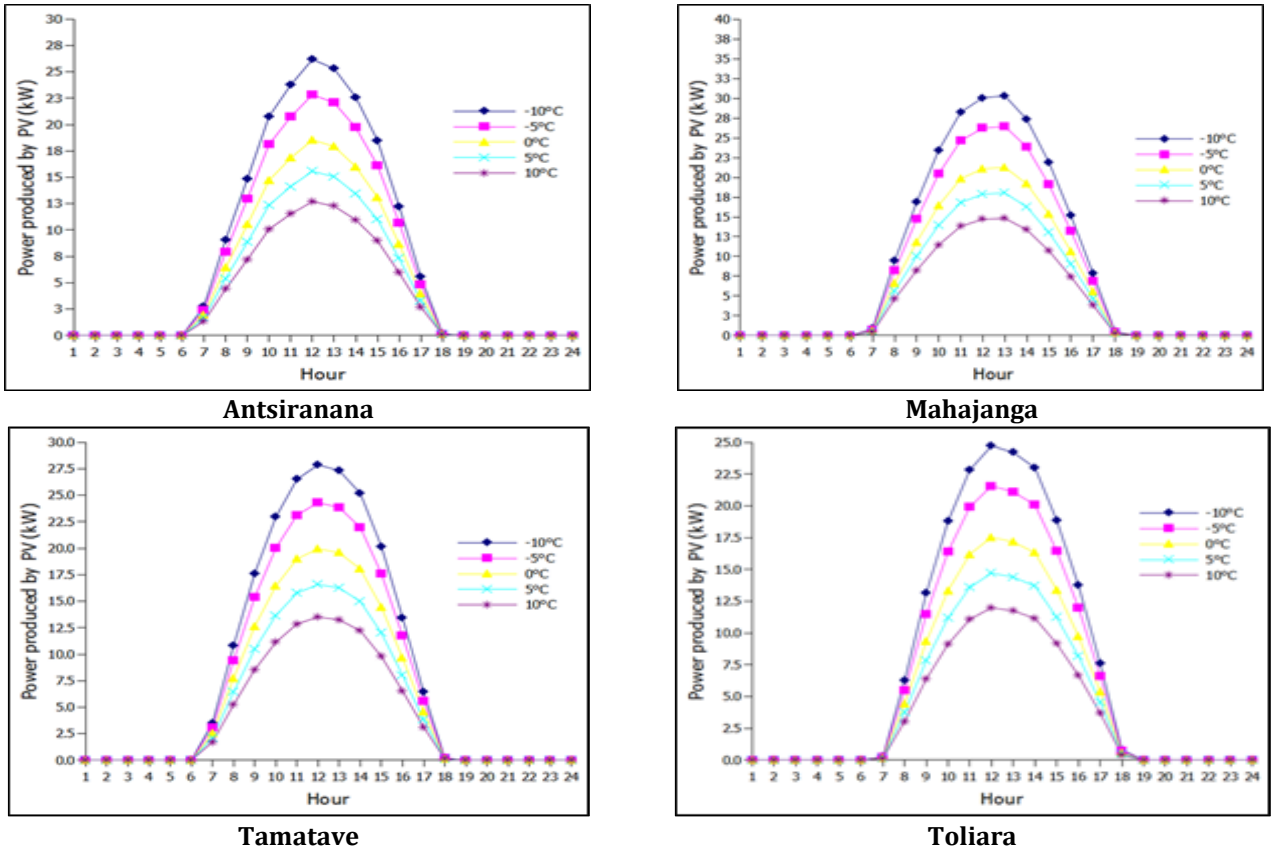

Figure 15 Hourly variation of the PV power for an evaporation temperature variation 0 ° C, -10 ° C, 10 ° C, -5 ° C, 5 ° C and 10 ° C for the first day of April for the selected cities

4.7. Overall system performance evaluation

Taking into account, the values of the total thermal load of the building and the photovoltaic power calculated from January to December, the overall monthly yields of the SE-VCR system are shown in Table 9. It was found that the overall performance of the installation also varies with the season. During the hot season, the COPs have a higher value. So, we can conclude that our SE-VCR system will have better returns for the months of March, April, October, November and December, with a maximum value of 52.1% in the month of April.

Table 8 Global system efficiency for evaporating temperature at 0 ° C for the selected cities

City	Overall efficiency of the installation	Jan	Feb	Mar	Apr	May	Oct	Nov	Dec
Antsiranana	[-]	43.08	42.16	42.45	44.41	45.57	45.8	45.17	42.6
Mahajanga	[-]	0.487	0.498	0.513	0.521	0.483	0.512	0.52	0.511
Toliara	[-]	43.3	41.9	43.5	45.17	47.18	46.53	46.26	43.08
Tamatave	[-]	43.42	42.78	42.44	43.16	44.43	45.47	44.12	43.16

Noel et al[17] found an overall system efficiency ranges from 17 to 35% while we found an overall efficiency ranges from 42.16 to 52.1%. Our result has a lot of advantage over the study made by Noel et al.[18]

5. Conclusion

In this research, we evaluated the performance of the vapor compression solar refrigeration system for the different climatic zones of Madagascar.To this end, on the 5 cities selected, the various hourly parameters such as the hourly loads of the building, the power of the compressor, condenser, evaporator and the power of the panel were determined. In addition, the coefficient of performance evaluation of this system in each selected city was evaluated in this research. It is very important to note that the SE-VCR system presents a good coefficient of performance for the city of Antsiranana, Mahajanga, Toliara and Tamatave while for the city of Antananarivo the use of this system is not very interesting because of its meteorological condition. For these 4 cities, the coefficient of performance varies from around 3.3 to 4.43 for an evaporation temperature Te = 0 ° C. And the compressor power ranges from 5.66 to 7.The peak power of a single photovoltaic generator used is 400Wp and a supply voltage of 24V. The overall efficiency of the installation varies from 0.4216 to 0.521.

This study is based on meteorological data obtained with Meteonorm software. The climatological analysis of the 4 cities allows us to conclude that they have a favorable climate for the system conventional vapor compression powered by solar energy. On the other hand, it is necessary to carry out further studies to come in order to properly refine the final technical parameters of the SE-VCR system on the one hand; and carry out measurements on the ground at the site.

Compliance with ethical standards

Acknowledgments

We acknowledge the local communities of survey districts for sharing their knowledge.

Disclosure of conflict of interest

No conflict of interest between the authors.

Nomenclature

C: heat input for one occupant (kW);
COP: Coefficient of performance [-];
D: Diameter (m)
Ec: Total energy consumed by the compressor for 24 hours in (kWh);
Ei: Hourly energy consumed by the compressor (kWh)
Epv: Energy produced by PV in kWh;
F: solar radiation area factor [-];
gv: reduction factor [-];
h: mass enthalpy in [kJ / kg];
Is: Solar radiation perpendicular to the surface of the PV (1kW / m^2);
K: Heat exchange coefficient (W / m^2.C);
L: piston stroke
m: mass flow rate of refrigerant (kg / s);
N: number of revolutions (rpm)
n: number of occupants;
P: Power of a lamp (W)
p: pressure (bar);
PV: Photovoltaic panel;
Q: Heat input (kW);
qv: volume flow (m3 / h)
Rb: Battery efficiency [-];
Ri: Efficiency of the installation [-];
R: Absorbed solar radiation (W / m^2);
S: Surface in (m^2);
T: temperature (° C);
Z: number of cylinders;
Wcr: Peak power of the panel in (kWp)

Greek symbol

α : Absorption coefficient [-];
ω : Relative humidity (g / kg dry air);
ν_1 : Mass volume (m3 / kg);
ε : efficiency [-];

Index

Cal: calorific
c: condenser;
ev: evaporator;
eff: effective
cp: compressor;
ray: radiation;
m: walls;
p: wall;
v: vitreous;
sr: sensitive by air renewal;
is: isentropic;
e: exterior;
g: global;
i: interior;
ins: installation
Soc: sensible heat by an occupant;
Loc: latent heat;
S: sensitive;
L: latent.

References

[1] IPCC. Climate change 2014: Synthesis report. Contribution of Working Groups I, II and III to the Fifth Assessment Report of the Intergovernmental Panel on Climate Change [Edited by the core editorial team, RK Pachauri and LA Meyer]. IPCC, Geneva, Switzerland. 2014; 161.

[2] Kyoto Protocol to the United Nations Framework Convention on Climate Change, FCCC / INFORMAL / 18 GE.9860500 (E).

[3] L GRIGNON-MASSE. Development of a cost-benefit analysis methodology to assess the potential for reducing environmental impacts linked to summer comfort: case of stationary room air conditioners in mainland France, thesis defended on May 20 2010 at the Ecole des Mines de Paris.

[4] D Clodic, Zero leakage. limitation of fluid emissions, 203 pages, Publisher: Pyc Livres. 1997.

[5] ADEME, key figures for building, energy, environment, 2010 editions.

[6] MAOUEL HAFIDHA, MOHAMMEDI KAMAL, YAMANI NORDINE, LEBIK SLIMANE. Contribution to the modeling and simulation of an absorption solar installation.

[7] Wu X. Polycrystalline thin film solar cells with high CdTe efficiency. Solar energy. 2004; 77: 803-814.

[8] Ayman Jamal Alazazmeh and Esmail M Mokheimer. Review of solar cooling technologies in Journal of Applied Mechanical Engineering. 2015.

[9] DS Kim, CA Infante. Ferreira Solar Refrigeration Options - A Review of International Leading Refrigeration

[10] Agnimoan Constant ALIHONOU and alt in 2019 made the bibliographical synthesis on Solar absorption air conditioning, mode of operation and description of the different elements of a solar air conditioning unit in the world. 2019.

[11] C Monne. and alt in 2009 did a study on the Stationary Analysis of a solar absorption LiBreH2O refrigeration system. 2009.

[12] Assilzadeh F. and alt in 2005 did the study on the Simulation and optimization of a Lithium Bromide (LiBr) solar absorption cooling system with evacuated tube collectors. 2005.

[13] Maher Shehadi in 2020 did the solar cooling system optimization study. 2020.

[14] Olivier Marc and alt in 2011 made the study on the Modeling and experimental validation of the solar loop for absorption solar cooling system using double glazing. 2011.

[15] Syed and alt in 2003 did a study on A new experimental study of a solar cooling system in Madrid. 2003.

[16] Riffat S, Xiaoli M. Thermoelectrics: a review of current and potential applications. Applied Thermal Engineering. 2003; 23: 913 -935.

[17] Noël Djonyang et al in 2012have shown that the production of cold from this energy source is possible.

[18] Noël Djongyang, René Tchinda, Donatien Njomo. Estimation of selected comfort parameters for sleeping environments in the dry tropical region of sub-Saharan Africa. 2012.

[19] Riffat S, Xiaoli M. Comparative study of thermoelectric air conditioners versus vapor compression and absorption air conditioners. Applied Thermal Engineering. 2004; 24: 1979-1993.

[20] Mehmet Bilgili in 2011 Hourly simulation and performance of the solar electricity-steam compression refrigeration system for the city of Adana in Turkey. 2011.

[21] Armand Noël, Ngueche Chédop, et al. Modeling the performance of a solar electric vapor compression refrigeration system in dry tropical regions.

[22] Todd Otanicar, Robert A. Taylor, Patrick E. Phelan. Prospects for Solar Cooling-An Economic and Environmental Assessment. Solar energy. 2012; 86(5): 1287– 1299.